npj | flexible electronics

www.nature.com/npjflexelectron

ARTICLE OPEN

Check for updates

Scalable and eco-friendly flexible loudspeakers for distributed human-machine interactions

Yucong Pi[1,4], Qiutong Liu[2,4], Zhaoyang Li[1], Dazhe Zhao[1], Kaijun Zhang[1], Zhirui Liu[2], Bingpu Zhou[3], Iek Man Lei[1], Yuan Ma[2,5]✉ and Junwen Zhong[1,5]✉

Flexible loudspeakers that can be easily distributed in the surrounding environment are essential for creating immersive experiences in human-machine interactions, as these devices can transmit acoustic information conveniently. In this paper, we present a flexible electret loudspeaker that offers numerous benefits, such as eco-friendly, easy fabrication, flexible customization, strong durability, and excellent outputs. The output sound pressure level (SPL) and frequency response characteristic are optimized according to the simulation and experiment results. At a distance of 50 meters, a large-size loudspeaker (50×40 cm^2) can produce an average SPL of 60 dB (normal SPL range of human voices is between 40 to 70 dB). The frequency response of our loudspeaker is high and relatively consistent up to 15 kHz, which covers the normal frequency range of human voices (<8 kHz). As demonstrated in this work, our loudspeakers can be used for scalable applications, such as being integrated with curtains or hung up like posters, offering a promising and practical solution for creating better human-machine interaction experiences.

npj Flexible Electronics (2023)7:45 ; https://doi.org/10.1038/s41528-023-00278-9

INTRODUCTION

The increasing development of human-machine interaction has led to a growing demand for electronics to disseminate information[1–6]. Of the five human senses[7] (i.e., vision, audition, gustation, olfaction, and touch) machines are most adept at providing visual and auditory experiences[8–11]. Loudspeakers, as vital hardware for transmitting acoustic information, are crucial to creating immersive experiences in applications such as augmented reality and virtual reality[12–15]. The rise of the Internet of Things (IoT) and web 3.0 has rendered centralized and single-sourced audio devices insufficient for delivering complex and context-specific audio effects[16]. To address this need, the industry is increasingly turning to distributed loudspeakers, which can be conveniently and labor-savingly applied in concerts. For large-scale IoT applications, it is essential to consider factors such as production and recovery costs, biodegradability, affordability, customizability, and scalability. In this regard, flexible and eco-friendly loudspeakers are more suitable for distributed applications on various object surfaces[17–19], as they are scalable and can create an immersive environment without being rigid or bulky.

Flexible loudspeakers are typically powered by electrostatic[6,14,19,20], piezoelectric[10,13,21–24], or thermoacoustic[17,25–28] transductions. Electrostatic flexible electret loudspeakers, in particular, offer structural simplicity, light weight, ease of production, and cost-effectiveness, making them ideal for human-machine interactive applications[29]. Although traditional rigid electret loudspeakers have been around for decades[30], the development of flexible electret loudspeakers has not been as rapid. A few flexible electret loudspeakers that currently exist use fluorocarbon polymers such as polytetrafluoroethylene (Teflon, PTFE)[31], fluorinated ethylene propylene (FEP)[32], and polypropylene (PP)[33]. While these polymers show promising performance, they are not biodegradable and not eco-friendly. Large-scale production and application of these loudspeakers could therefore pose a threat to the environment, leading to electronic waste problems or increased recovery costs. As such, developing an eco-friendly flexible electret loudspeaker holds significant commercial and environmental potential.

In this work, we present an eco-friendly flexible electret loudspeaker that utilizes polylactic acid (PLA) electret film, paper substrates, and carbon electrodes. PLA is a thermoplastic biopolymer that can be extracted from corn, potato starch, cassava root, or sugar cane[34]. It is biodegradable, biocompatible, and highly moldable, with excellent mechanical strength[35,36]. Moreover, PLA has been demonstrated to be an excellent electret material capable of storing a significant amount of electrostatic charges for an extended period[37–39], making it possible for PLA films to serve as the central diaphragm within the loudspeakers. Paper and carbon are both widely recognized as eco-friendly materials[40,41]. A degradation test shows that the entire loudspeaker decomposes significantly after 227 days. The key innovations of our loudspeaker include: (1) material and structure optimization, as validated by experimental and simulation results, improves the output sound pressure level (SPL) and frequency response characteristics of the loudspeaker, a rectangular loudspeaker with dimensions of 50×40 cm^2 can generate an SPL of 60 dB even at a distance of 50 meters away (significantly heard by human), and a high and relatively consistent SPL response is obtained up to 15 kHz, covering the typical frequency range of human voices (<8 kHz)[42]; (2) under root-mean-square voltage (Vrms) of 70.7 V, our loudspeaker has a high sensitivity of 0.444 mPa V^{-2} cm^{-2}, which is rather superior among reported electrostatic and piezoelectric flexible loudspeakers (Supplementary Table 1); (3) the shape of the loudspeaker can be easily customized, and the output performance is not impacted by the device's shape; (4) the flexibility is demonstrated by the uniform SPL directivity of a rolled

[1]Department of Electromechanical Engineering and Centre for Artificial Intelligence and Robotics, University of Macau, Macau SAR 999078, China. [2]Department of Mechanical Engineering and Research Institute for Intelligent Wearable Systems, The Hong Kong Polytechnic University, Hong Kong, China. [3]Joint Key Laboratory of the Ministry of Education, Institute of Applied Physics and Materials Engineering, University of Macau, Avenida da Universidade, Taipa, Macau 999078, China. [4]These authors contributed equally: Yucong Pi, Qiutong Liu. [5]These authors jointly supervised this work: Yuan Ma, Junwen Zhong. ✉email: y.ma@polyu.edu.hk; junwenzhong@um.edu.mo

loudspeaker, and the durability is exhibited by 11 h of continuous operation for both flat and rolled configurations; (5) as demonstrated, our loudspeakers can be integrated behind curtains to replace traditional rigid speakers, enhancing space utilization, they can also be hung up like posters, playing music loudly and clearly to create an immersive experience; and (6) to enhance portability, we have designed a self-made micro-voltage amplifier that can drive the loudspeakers to play audible audio in any environment, the sound wave and spectrogram are very similar to the original audio and those from mobile phones.

RESULTS AND DISCUSSION

Design strategy and typical features

As shown in Fig. 1a, our proposed flexible loudspeaker for distributed human-machine interaction can be integrated behind the curtain or hung casually on the wall like a poster to create an immersive experience. The detailed fabrication process of the loudspeaker is shown in Supplementary Fig. 1 and the Methods. The loudspeaker is a three-layered structure (Fig. 1b), with perforated paper substrates coated with carbon electrodes on one side and a polylactic acid (PLA) electret film as the main diaphragm in the middle layer. The material characterizations of the fabricated PLA film are performed. The Fourier Transform Infrared Spectroscopy (FTIR) of the fabricated PLA film shows the typical absorption peaks of PLA (Supplementary Fig. 2). The measured Young's modulus and relative dielectric constant of fabricated PLA film are ~1194 MPa (Supplementary Fig. 3) and 2.2 (Supplementary Fig. 4 and Supplementary Discussion), respectively. The eco-friendly carbon electrode is evenly spread on one side of the paper by hand drawing with a pencil, resulting in resistance values of ~400 Ω between the center and boundaries of a circular surface area of 16 cm^2 (Supplementary Fig. 5). The diameter of the perforation holes on the paper substrates and the distance between the hole centers are set at 1.2 and 4 mm, respectively, unless stated otherwise. The cross-sectional SEM image in Fig. 1c displays the structure of a typical loudspeaker. The top substrate, bottom substrate, and PLA film have thicknesses of 38, 437, and 80 μm, respectively, and the overall thickness of the device is ~700 μm, including the air gap thickness. In the design, double-sided tape with thickness of ~70 μm is applied to the edge and center of the device to ensure sufficient spacing between electrodes and PLA, thereby preventing any contact that may affect the audio performance of the loudspeaker. Further, Fig. 1d illustrates that the double-sided tape in the shape of fractal curve[43] is used as the spacer inner the large-size loudspeaker to improve the frequency response. However, it should be noted that if the spacing between electrodes and PLA is too large, the loudspeaker's performance may be compromised. Therefore, a spacer thickness of 70 to 140 μm generated by one or two layers of double-sided tape is chosen.

As a kind of electret and biodegradable polymer, PLA is an ideal choice for the main diaphragm of our proposed loudspeaker thanks to its eco-friendliness and its capability to store abundant electrostatic charges for a long time. After the PLA film is polarized using the Corona charging method[36], the negative and positive charges on the two surfaces generate a high surface potential as a built-in electrical field (E_{in}). When combined with the external electrical field (E_{out}) from the AC driving voltage, the loudspeaker vibrates to release sound, and the vibration is controlled by the AC driving voltage (Fig. 1b). The surface potential is equivalent to the effect of a DC bias voltage, which can reduce the AC driving voltage[44] or increase the SPL outputs when the driving voltage is given, as proved in Supplementary Fig. 6. The PLA film is fabricated by hot-pressing and quenching processes, which effectively increases the surface potential (Supplementary Fig. 7). The stable negative and positive surface potential values of PLA film used in this work are ~ −320 V and +310 V, respectively. When driven by a sinusoidal signal with 70.7 Vrms at 100 Hz, the vibrating displacement of a loudspeaker with a typical design (Fig. 1c) is measured using a laser Doppler vibrometry (LDV) (Supplementary Fig. 8). From the corresponding vibrating displacement results (Supplementary Fig. 9), a peak-to-peak displacement of roughly 5 μm at the location of the loudspeaker with max displacement is observed. This proves the significant vibration of our loudspeaker. The vibrating displacement versus driving frequency up to 20 kHz is also measured (Supplementary Fig. 10), indicating a reduction in vibrating displacement with increasing driving frequency, which remains roughly stable when the frequency is higher than 5 kHz. Figure 1e shows the vibrating displacement field of a circular-shaped loudspeaker. The vibrating displacement near the center is the most significant, matching well with the numerical results obtained by COMSOL Multiphysics, as shown in Supplementary Movie 1.

Our flexible loudspeakers are easily customizable in terms of shape and size, as both PLA film and paper substrates can be easily cut to the desired shape. The shapes of the loudspeakers used in experiments are mainly circular and rectangular, and more complex shapes are achieved in Supplementary Fig. 11, with additional sizes shown in Supplementary Fig. 12. Figure 1f displays a large-size loudspeaker (50×80 cm^2) in a rectangular shape, with a power density of less than 0.03 mW cm^{-2} over the entire range of audible frequencies, driven by a voltage of 70.7 Vrms (Supplementary Fig. 13). Compared to traditional flexible loudspeakers, our loudspeakers are based on biodegradable and pollution-free raw materials, eliminating electronic waste issues at the end of their product life cycle. Our loudspeakers can cover all required surfaces, without the limitation that recovery costs increase with area. Figure 1g depicts the degradation process of our eco-friendly loudspeaker. Obvious degradation, particularly the degradation of PLA film, is visible after incubating the device for 227 days, with the percentage of biodegradation of 63.8% (Supplementary Fig. 14). The temperature and humidity of the incubator are set to 60 °C and 100% RH, respectively, to accelerate the degradation process.

Simulation for key parameters optimization

In order to understand how different design parameters affect the performance of the loudspeaker, we develop axisymmetric and three-dimensional multiphysics finite element models to evaluate the electrostatic field, vibrating displacement, and induced sound pressure level (SPL) using a fully coupled method. The simulation is conducted in a spherical air domain with a perfect matching layer that encloses the entire device (Supplementary Fig. 15). The geometry designs for the loudspeakers used in the simulation, including configurations with and without holes on the paper substrates, are illustrated in Fig. 2a. The electrostatic field, vibrating displacement, and SPL response under a typical voltage of 70.7 Vrms at 6 kHz are shown in Fig. 2b. The simulation results indicate that when an external electrical field is applied to the device, the SPL response is quite uniform in the surrounding space of the loudspeaker, even though the vibrating displacement is not uniform (matching the experimental results in Fig. 1e). We further simulate the SPL response of the loudspeakers subjected to driving voltage amplitudes up to 100 Vrms, considering the key design parameters, including the thickness of paper substrates (under a frequency of 6 kHz), the surface potential of PLA electret (under a frequency of 6 kHz), and the holes on paper substrates (diameter of 1.2 mm, distance between the centers of the holes of 4 mm, under a frequency of 10.42 kHz). For the simulation on the effect of the thickness of paper substrates and the surface potential of PLA electret, we use axisymmetric models without holes on the paper substrates to simplify the calculation. It should be noted that the general simulation results of configurations with

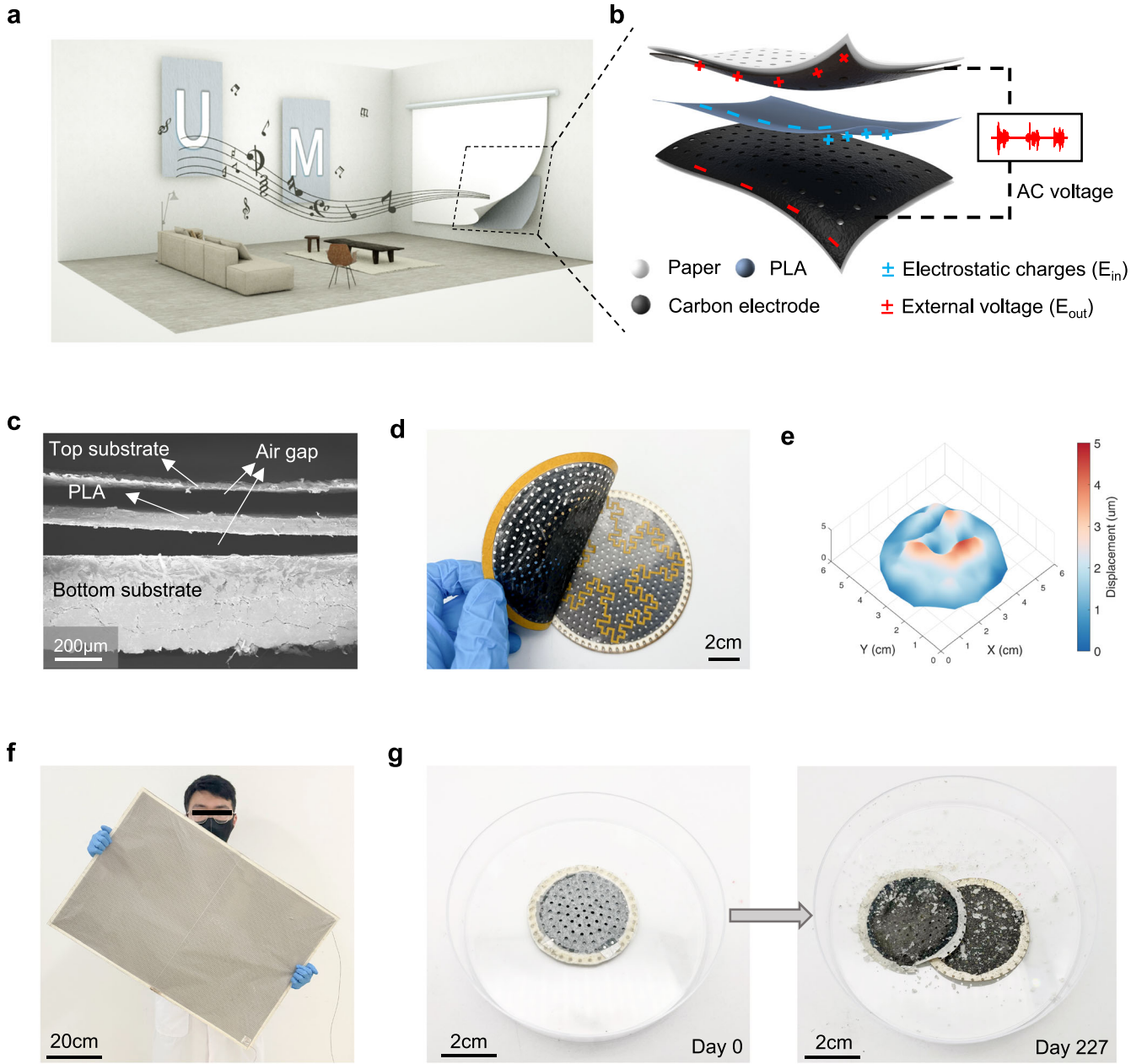

Fig. 1 Design strategy and typical features of the eco-friendly flexible electret loudspeakers. a Concept diagram of the application scenario. **b** Diagram illustrating the device structure of the loudspeaker and the electricity-sound conversion principle. **c** Cross-sectional SEM image of a typical loudspeaker (scale bar, 200 μm). **d** The double-sided tape spacer in the shape of fractal curve is placed inside the large-size loudspeaker (scale bar, 2 cm). **e** Vibrating displacement distribution of a circular-shaped loudspeaker measured by the LDV, when driven by a voltage of 70.7 Vrms at 100 Hz. **f** Photo of a rectangle-size loudspeaker in size of $50 \times 80\ cm^2$ (scale bar, 20 cm). **g** Photos illustrating the degradation process of a loudspeaker (scale bar, 2 cm).

and without holes are similar, making the simplified simulation reasonable and able to indicate the direction for design optimization.

Simulation results in Fig. 2c–e lead to the following conclusions: (1) a thin top substrate and a thick bottom substrate are preferred for larger SPL output; (2) higher surface potential on the electret can enhance the SPL response; (3) holes on substrates assist in releasing the sound pressure. These conclusions guide the design optimization of the loudspeaker for better performance.

Experiment characterizations for key parameters optimization

The experimental setup shown in Fig. 3a is designed to measure the influence of key design parameters on the SPL response of the loudspeakers with respect to the driving voltage. Circular-shaped loudspeakers with an area of 16 cm^2 are mounted on a frame in a self-made small soundproof shed, and a multifunctional noise analyzer is positioned 5 cm away from the center of the loudspeaker, as illustrated in Fig. 3b. The measurements are conducted at a fixed frequency of 6 kHz with the highest driving voltage of 100 Vrms.

The effect of the thickness of the top and bottom paper substrates is investigated, as shown in Fig. 3c, and the measurements are taken with a configuration that includes holes on the paper substrates. Six different loudspeakers with top and bottom paper substrates of respective thicknesses of 38, 103, or 437 μm (as shown in Supplementary Fig. 16) are tested for their

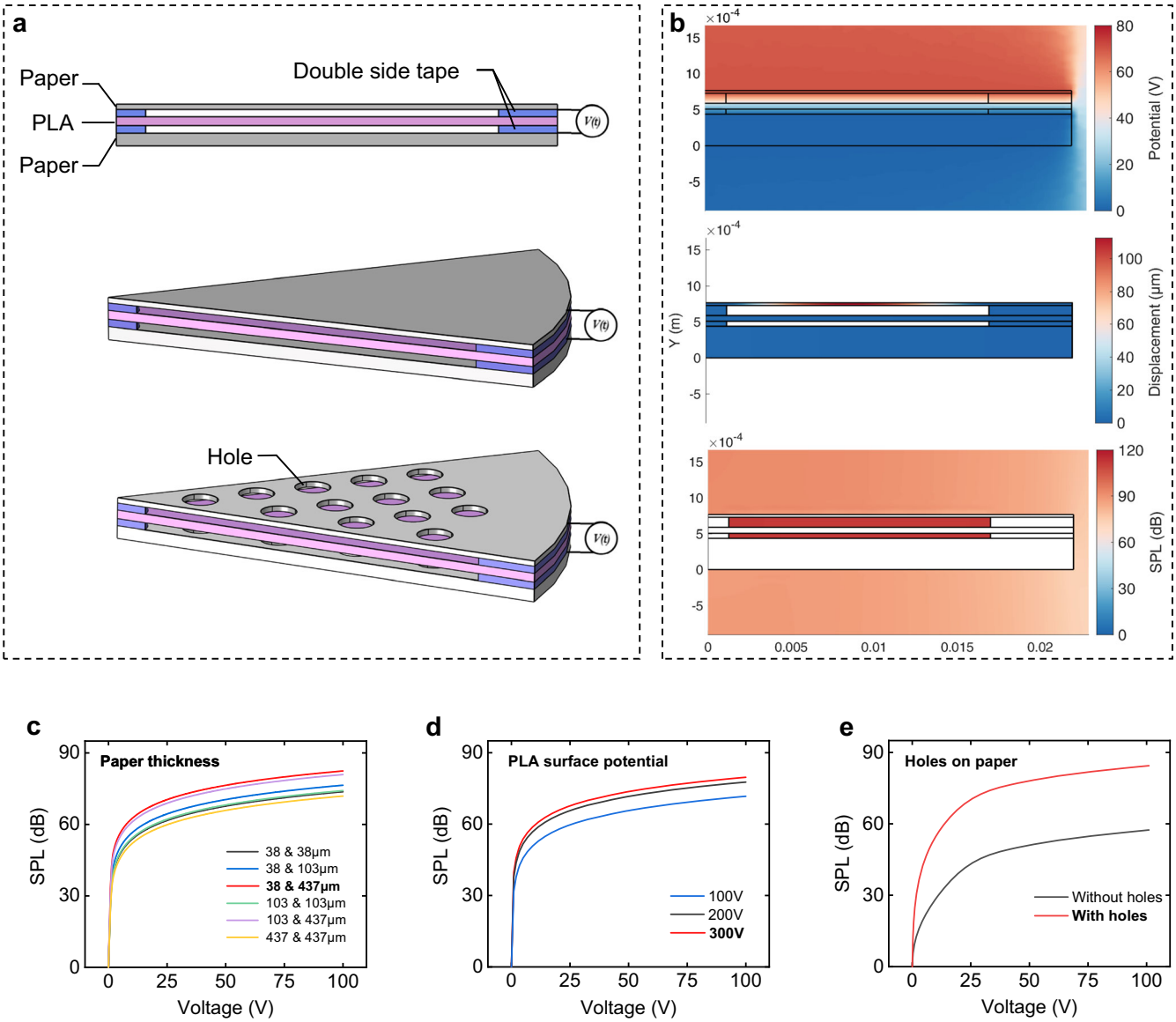

Fig. 2 Simulation for optimizing key parameters of the eco-friendly flexible electret loudspeakers. a The geometry of the finite element model. **b** Simulated electrostatic field, vibrating displacement, and SPL response at a driving voltage of 70.7 Vrms and frequency of 6 kHz. With a typical driving frequency, simulated SPL response as a function of driving voltage when considering key design parameters of (**c**) thickness of top and bottom paper substrates (simulated at 6 kHz), (**d**) surface potential of PLA electret (simulated at 6 kHz), and (**e**) hole on paper substrates (simulated at 10.42 kHz), respectively.

SPL response-driving voltage curves. The results indicate that the loudspeaker with the thinnest top substrate (38 μm) and the thickest bottom substrate (437 μm) exhibits the best SPL outputs. According to the simulation model, the top substrate and PLA film mainly contribute to the generated sound. A thin top substrate is therefore preferred because it can support larger deformation and allows for greater sound penetration. The thick bottom substrate ensures the stability of the entire device. The influence of the surface potential of PLA electret film (with average values of 100 V, 200 V, and 300 V) is measured with a configuration that including holes on the paper substrates (Fig. 3d). A high surface potential is found to be beneficial for increasing the output of the loudspeaker. It is worth noting that even at a driving voltage of only 17.7 Vrms, the SPL can reach up to 65 to 70 dB, which falls within the normal SPL range of human voices (between 40 to 70 dB[42]). The effect of the holes on the paper substrates is evaluated, as shown in Fig. 3e. The holes are found to assist in releasing the sound from the loudspeaker. Consequently, the loudspeaker with holes (with a diameter of 1.2 mm and a distance between the centers of the holes of 4 mm) on the paper substrates exhibits a better SPL response than the configuration without hole. A SPL of 80 to 85 dB at a driving voltage of 70.7 Vrms is achieved. Overall, the experimental results in Fig. 3 are generally consistent with the simulation results in Fig. 2.

The SPL measuring setup is used to further characterize the SPL response of the loudspeakers with respect to the driving frequency curves. In these measurements, the driving voltage is fixed at 70.7 Vrms, and the frequency varies within the human's hearing range between 20 Hz to 20 kHz[45,46]. Unless otherwise specified, the tested loudspeakers are circular-shaped with a size of 16 cm^2 and have holes on the paper substrates. The influence of the distance between hole centers on paper substrates (Supplementary Fig. 17) is shown in Fig. 4a. Within the frequency range below 15 kHz, the loudspeakers with a higher hole density (characterized by the distance between hole centers, *a*) generate higher SPL, reaching about 80 to 90 dB. However, higher hole

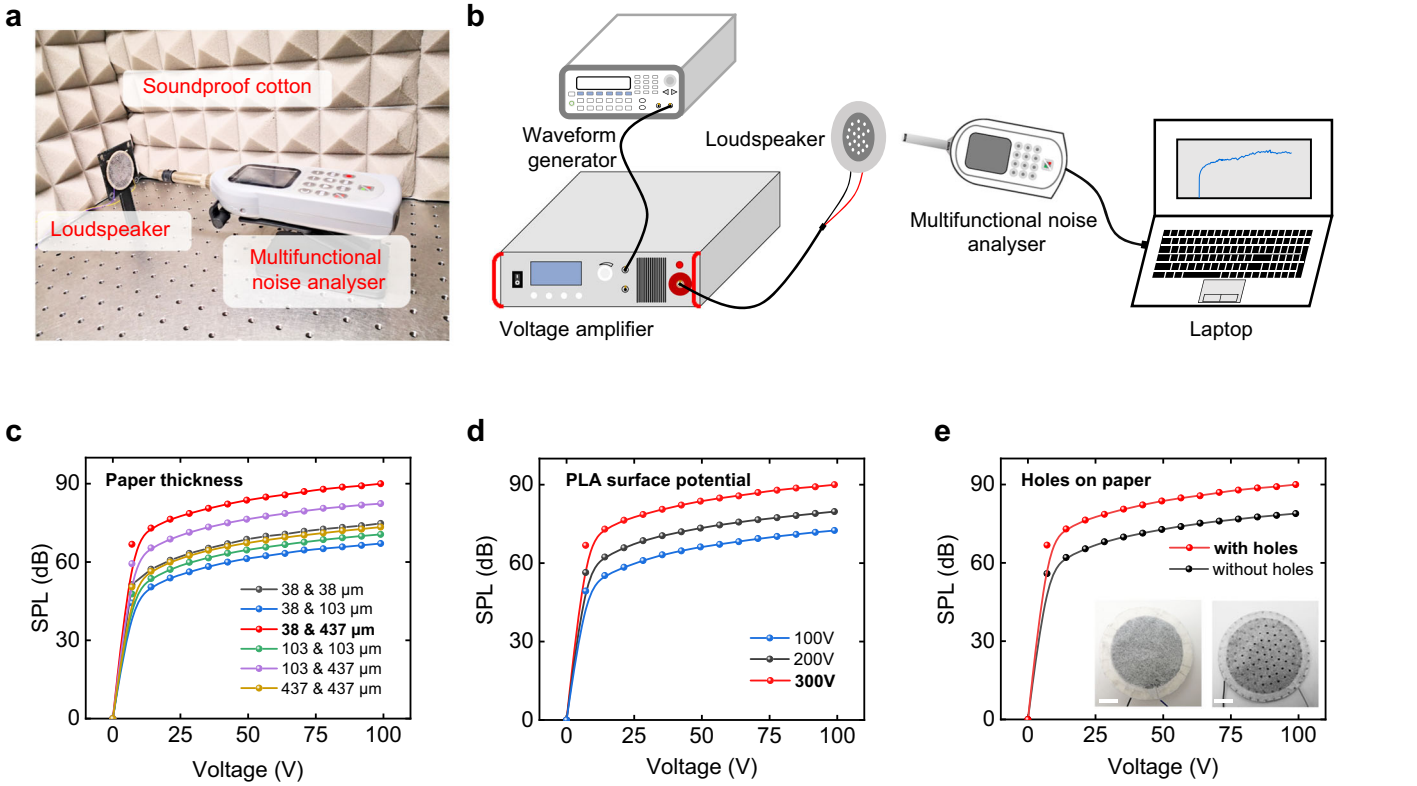

Fig. 3 Experimental measurement of SPL response with respect to driving voltage of the eco-friendly flexible electret loudspeakers. **a** Experimental setup for SPL measurement. **b** Diagram illustrating the details of the SPL measurement. **c**–**e** Measured SPL as a function of driving voltage considering different parameters when the driving frequency is 6 kHz. **c** Top and bottom paper substrates with different thicknesses, measured with configuration with holes on the paper substrates. **d** PLA electret films with different surface potentials, measured with configuration with holes on the paper substrates. **e** Paper substrates with and without holes, the insets show the photos of the loudspeakers with and without holes (scale bar, 1 cm). Under the same driving conditions, we test the SPL outputs of three devices and we show the typical outputs.

density compromises performance in the high-frequency range (15–20 kHz). On the other hand, since the normal frequency range of human voices is between 100 to 8000 Hz, loudspeakers with perforated holes are still preferable. Mechanical strength can also be a consideration for loudspeaker designs. For a prototype with $a = 2$ mm, structural failure can occur easily (Supplementary Fig. 18). Considering the SPL-frequency response under common scenarios and the mechanical strength of the device, a is chosen as 4 mm. The influence of the thickness of the top and bottom paper substrates is shown in Fig. 4b. The loudspeaker with the thinnest top substrate (38 μm) and the thickest bottom substrate (437 μm) generates the highest SPL under the frequency range of 20 Hz to 20 kHz. The influence of the surface potential and thickness of the PLA electret film on the SPL-frequency response is also studied. Figure 4c illustrates that the loudspeaker with the highest surface potential of an average value of about 300 V has the best SPL outputs under the entire testing frequency. Furthermore, the SPL-frequency response shows a distinct increase with the decrease of PLA electret film thickness (Supplementary Fig. 19 and Fig. 4d). This is because a thinner PLA diaphragm has a larger vibrating intensity under the same electrostatic force. On the other hand, the size of the loudspeakers (4, 9, or 16 cm^2) has a key effect on the performance (Supplementary Fig. 20). As expected, a larger loudspeaker has better SPL outputs, since larger devices represent larger point sources. In Fig. 4e, when comparing a loudspeaker with a size of 2000 cm^2 and one with a size of 16 cm^2, the 2000 cm^2-sized loudspeaker has a higher SPL at the frequency of 0–12 kHz, but a lower SPL at the frequency of 12–20 kHz. The measuring distance for loudspeaker with the size of 2000 cm^2 is 1 meter. The shapes of the loudspeakers (i.e., triangle, square, pentagon, hexagon, and circle) have negligible influence on the performance (Fig. 4f). With the same size of 16 cm^2, the SPL-frequency curves of the loudspeakers are similar, regardless of the shapes. This proves that our loudspeaker can be easily customized to serve various application scenarios.

Supplementary Table 1 compares the performances of our loudspeakers with the typically reported flexible loudspeakers based on electrostatic, piezoelectric, and thermoacoustic transductions in the literature[10,13,19,23,24,28,29,31,33,47–60]. Although electrostatic and piezoelectric flexible loudspeakers normally have good frequency response, their driving voltage is high (tens or hundreds of volts). By contrast, the performances of our eco-friendly flexible electret loudspeaker, such as driving voltage, output SPL, and sensitivity, surpass the reported electrostatic and piezoelectric flexible loudspeakers. Typically, our eco-friendly flexible loudspeaker has a high sensitivity of 0.444 mPa V^{-2} cm^{-2}. The driving voltage of thermoacoustic flexible loudspeakers is lower (can be as low as several volts). However, the sound generation is compromised in the low-frequency audible band[28].

Characterizations for flat and rolled loudspeakers

SPL directivity is a quantitative measure of the focusing of sound, indicating the proportion of sound energy directed toward different directions[19]. To study the variation of SPL outputs at any angle, the directivity of SPL is measured using two configurations (Supplementary Fig. 21): a flat loudspeaker with a surface area of 9 cm^2 and a rolled loudspeaker with a projection area of 9 cm^2. The experimental setups for SPL directivity

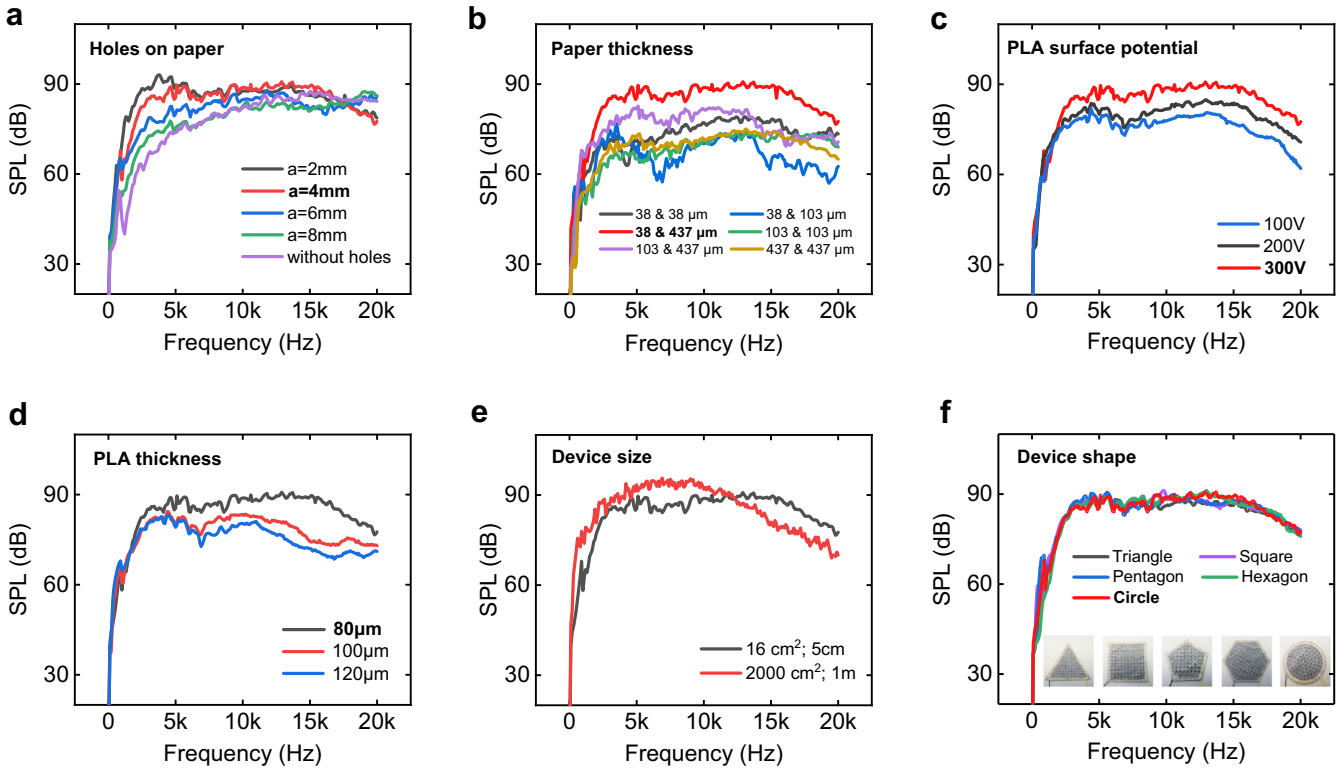

Fig. 4 Measured SPL-frequency response of the eco-friendly flexible loudspeakers. a–f Measured SPL as a function of frequency considering different design parameters when the driving voltage is 70.7 Vrms. Unless otherwise specified, the shape of a tested loudspeaker is circular, the size is 16 cm^2, and the device is the configuration with holes on the paper substrates. **a** Paper substrates with a fixed hole diameter of 1.2 mm and different hole densities, "*a*" represents the distance between the centers of two holes. **b** Top and bottom paper substrates with different thicknesses. **c** PLA electret films with different surface potentials. **d** PLA electret films with different thicknesses. **e** Loudspeakers with different sizes. **f** Loudspeakers with different shapes and the same area of 16 cm^2, the insets show the photos of the loudspeakers of triangle, square, pentagon, hexagon, and circle shapes. Under the same driving conditions, we test the SPL outputs of three devices and we show the typical outputs.

measurement of the two types of loudspeakers are shown in Fig. 5a, b. The loudspeakers are attached to a square-shaped or cylinder-shaped frame that can freely rotate 360°. A multifunctional noise analyzer facing the center axis of the frames takes measurements at a position of 5 cm away. The flat and rolled loudspeakers are driven at a fixed driving frequency of 6 kHz and a voltage of 17.7 Vrms, 53 Vrms, and 88.4 Vrms, and the SPL outputs for every 10° rotating angle interval are recorded. The SPL polar plots of the flat loudspeaker in Fig. 5c illustrate that rotation makes the projected area that generates sound energy directly toward the multifunctional noise analyzer smaller, thus reducing the resulting SPL. In addition, the SPL directivity results at different voltages have similar directivity patterns except for the SPL intensity. Figure 5d illustrates the SPL polar plots of the rolled loudspeaker. As the projected area is the same for every rotating angle, the rolled loudspeaker demonstrates omnidirectional performance. Furthermore, under a fixed driving voltage of 70.7 Vrms and frequencies of 500 Hz, 2 kHz, and 10 kHz, SPL directivity performances of flat and rolled loudspeakers are also tested. As shown in Supplementary Fig. 22, the results are similar to those of the cases of fixed frequency and variational voltage. The loudspeakers still work well after being rolled up several times. The SPL directivity test for the rolled loudspeaker proves the outstanding flexibility of our loudspeaker.

The attenuation of SPL with a distance of up to 30 cm for the two types of loudspeakers with a driving voltage of 70.7 Vrms and frequency of 6 kHz at a rotating angle of 0° is shown in Fig. 5e. With increasing distance, both the resulting SPL outputs decrease, and the two types of loudspeakers have similar amplitude-distance responses. The SPL is about 60 dB when the distance reaches 30 cm, which is not a low value and can be clearly heard. Moreover, the long-term output stability of the two types of loudspeakers is shown in Fig. 5f. During continuous 11 working hours at a voltage of 70.7 Vrms and frequency of 6 kHz, the SPL values at a distance of 5 cm and rotating angle of 0° remain stable at about 80 dB. Furthermore, after a flat loudspeaker is placed in lab conditions for 108 days, the SPL values are still almost the same as the initial ones. The excellent long-term output stability ensures the durability of our loudspeakers during real usage.

Demonstrated application for the loudspeakers

In the demonstration, audio signals are sent out by an audio signal source such as a laptop, mobile phone, or mp3 player. The NI data acquisition converts the audio signals into voltage signals, which are then amplified by the voltage amplifier to drive our loudspeakers (Supplementary Fig. 23 and Supplementary Movie 2). In Fig. 6a and Supplementary Movie 3, four 50×40 cm^2 rectangle loudspeakers are installed behind a curtain in a classroom and play a song. The flexibility of the loudspeakers allows them to fit well with the projection curtain, even during the rolling of the curtain. The integrated design of the loudspeaker and curtain has the advantage of effectively reducing space occupancy and providing good volume ceiling due to the feature of increasing volume with increasing area. In order to improve the attenuation of response in high-frequency band after the loudspeaker area is enlarged, the double-sided tape in the shape of fractal curve (Supplementary Fig. 24) is used as the spacer placed inside the large-size loudspeaker, which purpose is to

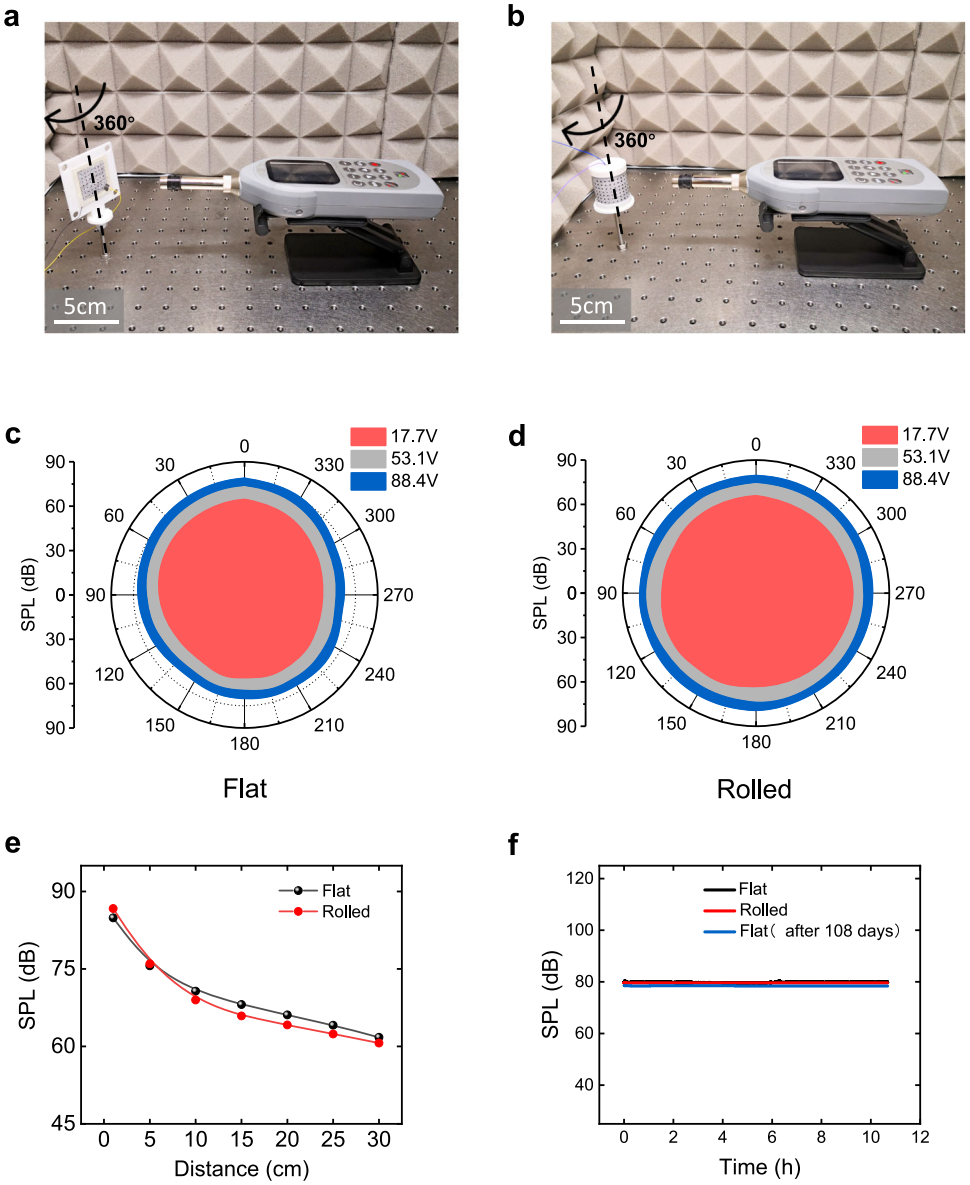

Fig. 5 SPL directivity, attenuation of SPL with distance, and stability of flat and rolled loudspeakers. a, **b** Experimental setup for SPL directivity measurement (scale bar, 5 cm). **a** Flat loudspeaker with a surface area of 9 cm^2. **b** Rolled loudspeaker with a fixed projected area of 9 cm^2. SPL polar plots under fixed driving frequency of 6 kHz and voltage of 17.7 Vrms, 53.1 Vrms, and 88.4 Vrms for (**c**) a flat loudspeaker and (**d**) a rolled loudspeaker. **e** Attenuation of SPL with distance up to 30 cm for the flat and rolled loudspeakers, under driving voltage of 70.7 Vrms and frequency of 6 kHz. **f** Output stability of flat loudspeakers (new one and after 108 days in lab conditions of ~ 25 °C and ~ 60%RH) and rolled loudspeaker under continuous 11 working hours, with driving voltage of 70.7 Vrms and frequency of 6 kHz.

isolate small-size loudspeakers within the large-size loudspeaker to compensate for response in high-frequency band. As expected, loudspeaker with the fractal curve spacer shows a better frequency response in Fig. 6b.

Furthermore, in Fig. 6c and Supplementary Movie 4, a rectangle loudspeaker (50 × 40 cm^2 in size) is placed at the end of a corridor, and the "Song of the University of Macau" can be clearly heard at a distance of 50 meters away. The SPL remains stable at around 60 dB. As the user gradually approaches the loudspeaker (Supplementary Movie 5), the intensity of the sound increases steadily, and it becomes evident that the sound increases as the distance from the loudspeaker decreases. For portability, we custom-design a micro-voltage amplifier (Supplementary Fig. 25) to drive our loudspeaker, with the circuit diagram and voltage-frequency response shown in Supplementary Figs. 26 and 27. The self-made micro-voltage amplifier only requires one 9 V battery, and the total size is just 3 × 4 cm^2, ensuring its portability. As shown in Fig. 6d, the NI data acquisition and voltage amplifier are replaced by the self-made micro-voltage amplifier system, which is then used to drive a loudspeaker (circular-shaped, 78 cm^2 in size). The played audio is recorded by a commercial microphone. In Fig. 6e, the sound wave and acoustic spectrogram of the original audio (top), audio played by a mobile phone (middle), and audio played by our loudspeaker (bottom) are shown. The specific audio is "University of Macau" in Chinese Mandarin, English, and Cantonese, respectively, as shown in Supplementary Movie 6. The sound wave pattern and spectrogram from our loudspeaker are very similar to the original audio and the ones from the mobile phone. The sound wave and acoustic spectrogram of "ABC song" from the mobile phone and our loudspeaker are also very similar (Supplementary Fig. 28). These results prove that the performance of our loudspeaker is as good as commercial loudspeakers.

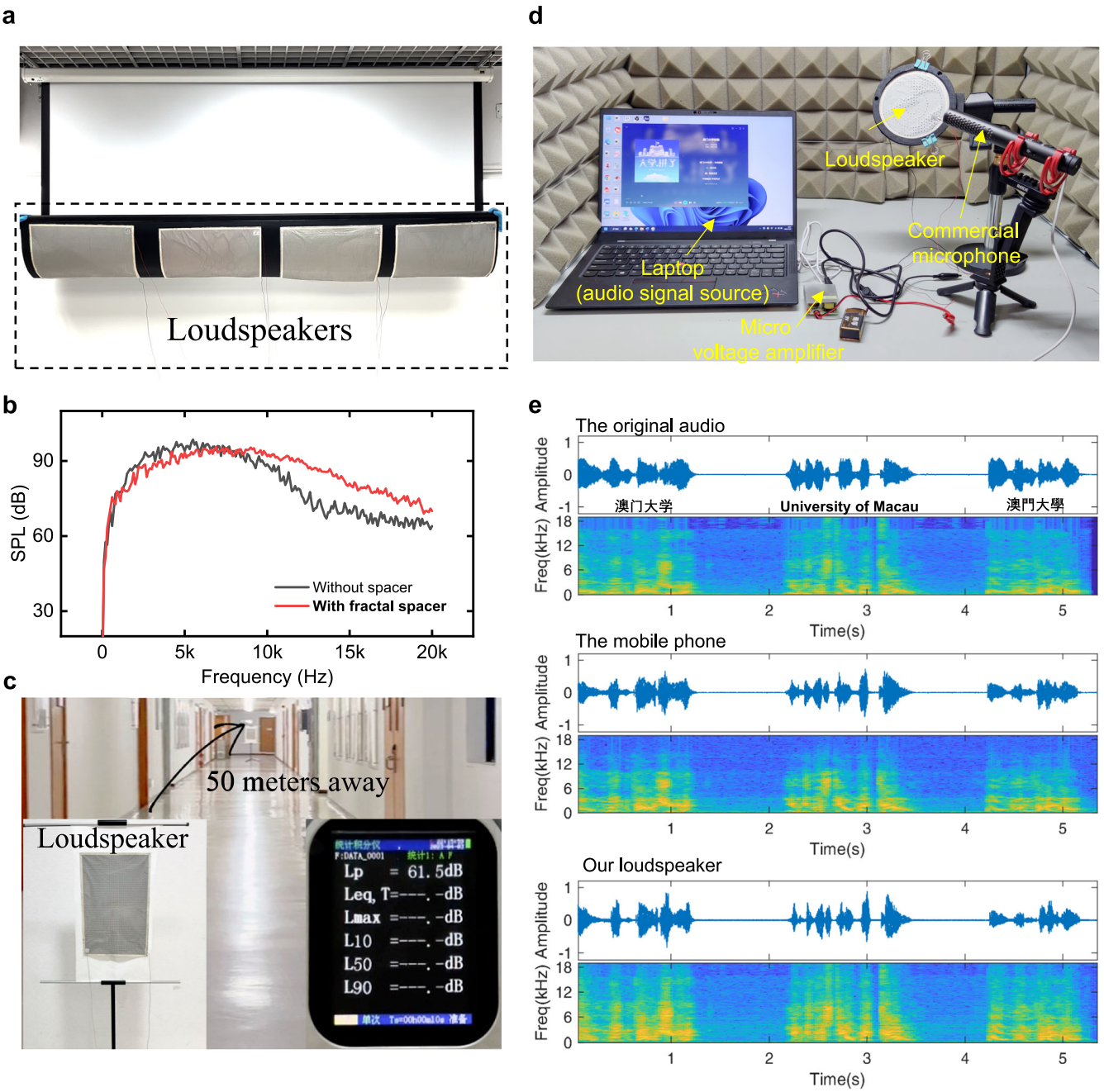

Fig. 6 Demonstrated application for the eco-friendly flexible loudspeakers. a Photo illustrating four rectangle loudspeakers (50×40 cm^2) playing music integrated behind the curtain. **b** Loudspeakers with or without fractal spacer. **c** Photo illustrating a rectangle loudspeaker (50×40 cm^2) playing music at the distance of 50 meters away. **d** Photo illustrating a loudspeaker driven by a self-made micro-voltage amplifier working with an audio signal source (laptop). **e** Sound wave and acoustic spectrogram of original audio of "University of Macau" (top), audio played by a mobile phone (middle), and audio played by our loudspeaker (bottom).

In summary, we propose a low-cost and eco-friendly flexible electret loudspeaker based on PLA electret film, paper substrates, and carbon electrodes, which are pollution-free raw materials. To achieve optimal performance, key design parameters are optimized through finite element modeling and experimental verification. Both simulation and experimental results indicate that a thin top substrate, thick bottom substrate, high surface potential of PLA electret, thin PLA film thickness, and appropriate hole density on paper substrates improve the SPL outputs. A rectangle-shaped loudspeaker with a size of 50×40 cm^2 can produce an SPL of 60 dB even at a distance of 50 meters. The SPL response of our loudspeaker is stable with driving frequency of up to 15 kHz, covering the normal frequency range of human voices (<8 kHz). Our loudspeaker's shapes are easily customizable, and the paper substrate and PLA film can be easily scissored without affecting output performance. The flexibility is verified by the uniform SPL directivity of a rolled loudspeaker, and the durability is demonstrated with stable outputs during 11 continuous hours of operation and after 108 days storage in lab conditions. As demonstrated, our loudspeakers can be integrated behind a curtain in the classroom or hung up like a poster in the corridor, providing good sound quality and volume while greatly improving space utilization compared to traditional loudspeakers. For portability, our loudspeakers can be driven by a micro-voltage

amplifier, producing audible audios with sound wave patterns and spectrograms similar to the original audio and ones played from a mobile phone. Future work to improve our eco-friendly flexible electret loudspeakers includes modifying PLA electret or developing new eco-friendly electret materials to improve surface potential and mechanical properties. Additionally, ensuring the durability of our loudspeakers in outdoor environments is another area for improvement.

METHODS

Fabrication of the eco-friendly flexible loudspeaker

The detailed fabrication steps of the loudspeaker are shown in Supplementary Fig. 1. Step I-cutting holes on paper substrates: the laser module (power of 1.6 W) of a Snapmaker A350T 3D printer is used to cut regular circle holes with diameter of 1.2 mm on the paper substrates with thickness of 38, 103, or 437 μm, and the distance between the center of two holes is set as 2, 4, 6, or 8 mm. Step II-fabricating electrodes: carbon electrode is evenly spread on one surface the paper substrates by a pencil with a hardness class of 6B. Step III-attaching external conductors: conductive wires are attached to the edge on the electrodes. Step IV-fabricating PLA electret film: A PLA disc with diameter of 20 mm and thickness of 0.8 mm is fabricated by a Snapmaker A350T 3D printer with white PLA filament as raw material, the PLA disc is then hot pressed into thin film with weight of 14 kg for 5, 8, or 10 min under temperature of 220 °C, the obtained PLA films with thickness of 80, 100, or 120 μm are quenched in water immediately or after cooling to set temperature (100 °C) before quenching. Step V-Adhering PLA film: A PLA electret film is adhered to the electrode surface of one paper substrate (defined as bottom substrate), with boundaries fixing with double-sided tape. Step VI-Corona charging: The PLA film is faced to the Corona needle with a distance of 5 cm, the high voltage up to −16 kV is applied by a DC power supply (DW-N503-4ACD2, Tianjin Dongwen), the charging time is 5 min to fully inject electrostatic charges (surface potential value of ~ −300 V). Charging voltage values are reduced to −12 kV and −8 kV for getting stable surface potential values of ~ −200 V and ~ −100 V, respectively. When fabricating large-size devices, the PLA film is partitioned and sequentially polarized one by one (Supplementary Fig. 29). Step VII-assembling device: the electrode surface of another paper substrate (defined as top substrate) is faced to the PLA film of bottom substrate, with boundaries fixing with double-sided tape. Step VIII-fabricated device: flexible loudspeakers with customized shapes and sizes are obtained.

COMSOL Multiphysics simulation

We simulate SPL-voltage and SPL-frequency responses using 2D and 3D finite element analysis in COMSOL Multiphysics. In the model, a stable state solution is first calculated for fully coupled solid mechanics, electrostatic force, and SPL. Then, the driving voltage is defined in the model with linear perturbation functions. The narrow region acoustic model is used for air gaps between the paper substrates and PLA. The simulation of the acoustic response for the loudspeakers is conducted by extracting the values of the absolute sound pressure field distributed in the air domain at a distance of 5 cm from the centre of the loudspeaker. To absorb the sound wave reaching the boundary and simulate an infinitely extended sound field propagation environment, we defined a perfectly matching layer with a diameter of 1 m. In specific, Supplementary Table 2 shows the geometrical structure parameters of the loudspeakers in the COMSOL simulation. Supplementary Table 3 provides the mechanical and electrical characterization of materials in the COMSOL simulation.

Characterization

The driving signals for loudspeakers are generated by a function generator (33210A, KEYSIGHT) or a NI USB 6341 data acquisition system and amplified 100 times by a power amplifier (ATA-7010, Aigtek) or a self-made micro-voltage amplifier working with any audio signal sources. A multifunctional noise analyzer (AWA6228+, AIHUA) is used to perform all sound pressure level data measurements, and the background noise is about 35 dB. The vibrating displacement of the loudspeakers is measured by a LDV (Vibro One, Polytec), with a range of 50 μm, a sensitivity of 25 μm V^{-1}, and a 30 Hz high-pass filter. The SEM images are probed by a high-resolution Field Emission Scanning Electron Microscope (Sigma FE-SEM, Zeiss Corporation). The surface potential values of the PLA electret films are measured using an electrostatic voltmeter (Trek 347). Fourier Transform Infrared Spectroscopy (FTIR) of the fabricated PLA film is measured by a FTIR Spectrometer (INVENIO, Bruker). Young's modulus of the fabricated PLA film is measured by a tensile machine (8010, CTM). The capacitance of PLA film is measured by a LCR meter (E4980AL, KEYSIGHT). The resistance values of carbon electrodes are measured by a Source Meter (2400, KEITHLEY).

DATA AVAILABILITY

The data that support the findings of this study are available from the corresponding author upon reasonable request.

Received: 6 June 2023; Accepted: 26 September 2023;
Published online: 07 October 2023

REFERENCES

1. Su, Q. et al. A stretchable and strain-unperturbed pressure sensor for motion interference-free tactile monitoring on skins. *Sci. Adv.* **7**, eabi4563 (2021).
2. Kim, J. et al. Wearable smart sensor systems integrated on soft contact lenses for wireless ocular diagnostics. *Nat. Commun.* **8**, 14997 (2017).
3. Tian, X. et al. Wireless body sensor networks based on metamaterial textiles. *Nat. Electron.* **2**, 243–251 (2019).
4. Shi, X. et al. Large-area display textiles integrated with functional systems. *Nature* **591**, 240–245 (2021).
5. Lee, S. et al. A transparent bending-insensitive pressure sensor. *Nat. Nanotech.* **11**, 472–478 (2016).
6. Keplinger, C. et al. Stretchable, transparent, ionic conductors. *Science* **341**, 984–987 (2013).
7. Serres, M. *The Five Senses: A Philosophy of Mingled Bodies* (Bloomsbury Publishing, 2008).
8. Mishra, S. et al. Soft, wireless periocular wearable electronics for real-time detection of eye vergence in a virtual reality toward mobile eye therapies. *Sci. Adv.* **6**, eaay1729 (2020).
9. Lee, J. et al. Stretchable skin-like cooling/heating device for reconstruction of artificial thermal sensation in virtual reality. *Adv. Funct. Mater.* **30**, 1909171 (2020).
10. Han, J., Lang, J. H. & Bulović, V. An ultrathin flexible loudspeaker based on a piezoelectric microdome array. *IEEE Trans. Ind. Electron.* **70**, 985–994 (2022).
11. Lee, S. et al. A high-fidelity skin-attachable acoustic sensor for realizing auditory electronic skin. *Adv. Mater.* **34**, 2109545 (2022).
12. Yang, Q. et al. Mixed-modality speech recognition and interaction using a wearable artificial throat. *Nat. Mach. Intell.* **5**, 169–180 (2023).
13. Shehzad, M., Wang, S. & Wang, Y. Flexible and transparent piezoelectric loudspeaker. *npj Flex. Electron.* **5**, 1–6 (2021).
14. Zhou, Q. & Zettl, A. Electrostatic graphene loudspeaker. *Appl. Phys. Lett.* **102**, 223109 (2013).
15. Xu, S. et al. Graphene–silver nanowire hybrid films as electrodes for transparent and flexible loudspeakers. *CrystEngComm* **16**, 3532–3539 (2014).
16. Wang, H., Chen, Z. & Xie, H. A high-SPL piezoelectric MEMS loudspeaker based on thin ceramic PZT. *Sens. Actuat. A Phys.* **309**, 112018 (2020).
17. Kang, S. et al. Transparent and conductive nanomembranes with orthogonal silver nanowire arrays for skin-attachable loudspeakers and microphones. *Sci. Adv.* **4**, eaas8772 (2018).
18. Zhang, Q. et al. Flexible multifunctional platform based on piezoelectric acoustics for human–machine interaction and environmental perception. *Microsyst. Nanoeng.* **8**, 1–13 (2022).

19. Li, W. et al. Nanogenerator-based dual-functional and self-powered thin patch loudspeaker or microphone for flexible electronics. *Nat. Commun.* **8**, 15310 (2017).
20. Chen, J.-L. & Chiang, D.-M. *A Novel Flexible Loudspeaker Driven by an Electret Diaphragm* (Audio Engineering Society, 2006).
21. Shehzad, M. & Wang, Y. Flexible and transparent flexoelectric microphone. *Adv. Mater. Technol.* **8**, 2200908 (2023).
22. Han, J., Saravanapavanantham, M., Chua, M. R., Lang, J. H. & Bulović, V. A versatile acoustically active surface based on piezoelectric microstructures. *Microsyst. Nanoeng.* **8**, 1–10 (2022).
23. Yildirim, A. et al. Roll-to-roll production of novel large-area piezoelectric films for transparent, flexible, and wearable fabric loudspeakers. *Adv. Mater. Technol.* **5**, 2000296 (2020).
24. Sugimoto, T. et al. PVDF-driven flexible and transparent loudspeaker. *Appl. Acoust.* **70**, 1021–1028 (2009).
25. Gong, S. et al. Hierarchically resistive skins as specific and multimetric on-throat wearable biosensors. *Nat. Nanotechnol.* **18**, 1–9 (2023).
26. Tao, L.-Q. et al. An intelligent artificial throat with sound-sensing ability based on laser induced graphene. *Nat. Commun.* **8**, 14579 (2017).
27. Tian, H. et al. Graphene-on-paper sound source devices. *ACS Nano* **5**, 4878–4885 (2011).
28. Jin, S. W. et al. A flexible loudspeaker using the movement of liquid metal induced by electrochemically controlled interfacial tension. *Small* **15**, 1905263 (2019).
29. Chen, Y.-C. et al. Tailoring the performance of flexible electret loudspeakers by varying cell actuator formation. *IEEE Trans. Dielectr. Electr. Insul.* **19**, 1094–1100 (2012).
30. Roberts, R. C. et al. Electrostatically driven touch-mode poly-SiC microspeaker. *IEEE Sens.* **1–3** 284–287 (2007).
31. Ko, W.-C. et al. Study and application of free-form electret actuators. *IEEE Trans. Dielectr. Electr. Insul.* **19**, 1226–1233 (2012).
32. Altafim, R. A. C. et al. Piezoelectrets from thermo-formed bubble structures of fluoropolymer-electret films. *IEEE Trans. Dielectr. Electr. Insul.* **13**, 979–985 (2006).
33. Dsouza, H. et al. Ferroelectret nanogenerators for loudspeaker applications: a comprehensive study. *J. Sound. Vib.* **468**, 115091 (2020).
34. Reddy, G. Altaf, Md., Naveena, B. J., Venkateshwar, M. & Kumar, E. V. Amylolytic bacterial lactic acid fermentation—a review. *Biotechnol. Adv.* **26**, 22–34 (2008).
35. Jiang, X. et al. *Poly (Lactic Acid): Synthesis, Structures, Properties, Processing, and Applications* (John Wiley & Sons, Inc., 2010).
36. Vraneva, A., Yovcheva, T. & Mekishev, G. Pressure effect on the polymer electret films. *IEEE Trans. Dielectr. Electr. Insul.* **20**, 1882–1886 (2013).
37. Galikhanov, M. F., Zhigaeva, I. A., Minnakhmetova, A. K. & Deberdeev, R. Y. Biodegradability of electret polymer materials. *Russ. J. Appl. Chem.* **81**, 1258–1261 (2008).
38. Guzhova, A. A., Galikhanov, M. F., Kuznetsova, N. V., Petrov, V. A. & Khairullin, R. Z. Effect of polylactic acid crystallinity on its electret properties. *AIP Conf. Proc.* **1767**, 020009 (2016).
39. Guzhova, A., Yovcheva, T. & Vraneva, A. Study of polylactic acid corona electrets. *Bulg. Chem. Commun.* **47**, 115–120 (2015).
40. Tobjörk, D. & Österbacka, R. Paper electronics. *Adv. Mater.* **23**, 1935–1961 (2011).
41. Pommier, S., Llamas, A. M. & Lefebvre, X. Analysis of the outcome of shredding pretreatment on the anaerobic biodegradability of paper and cardboard materials. *Bioresour. Technol.* **101**, 463–468 (2010).
42. Olson, H. F. *Elements of Acoustical Engineering* (D. Van Nostrand Company, Inc., 1940).
43. Lauwerier, H. & Lauwerier, H. A. *Fractals: Endlessly Repeated Geometrical Figures* (Princeton University Press, 1991).
44. Qiu, W. et al. A low voltage-powered soft electromechanical stimulation patch for haptics feedback in human-machine interfaces. *Biosens. Bioelectron.* **193**, 113616 (2021).
45. Rosen, S. & Howell, P. *Signals and Systems for Speech and Hearing*, Vol. 29 (BRILL, 2011).
46. Dunn, F., Hartmann, W., Campbell, D., Fletcher, N. & Rossing, T. *Springer Handbook of Acoustics* (Springer, 2015).
47. Ko, W.-C. et al. Use of 2-(6-mercaptohexyl) malonic acid to adjust the morphology and electret properties of cyclic olefin copolymer and its application to flexible loudspeakers. *Smart Mater. Struct.* **19**, 055007 (2010).
48. Chiang, H.-Y. & Huang, Y.-H. Vibration and sound radiation of an electrostatic speaker based on circular diaphragm. *J. Acoust. Soc. Am.* **137**, 1714 (2015).
49. Liao, H.-C. et al. On the improvement for charging large-scale flexible electrostatic actuators. *Proc. SPIE Int. Soc. Opt. Eng. Proc.* **7979**, 112–125 (2011).
50. Chiang, H.-Y. & Huang, Y.-H. Resonance mode and sound pressure produced by circular diaphragms of electrostatic and piezoelectric speakers. *Appl. Acoust.* **129**, 365–378 (2018).
51. Lee, C. S. et al. An approach to durable poly (vinylidene fluoride) thin film loudspeaker. *J. Mater. Res.* **18**, 2904–2911 (2003).
52. Hübler, A. C. et al. Fully mass printed loudspeakers on paper. *Org. Electron.* **13**, 2290–2295 (2012).
53. Yu, X., Rajamani, R., Stelson, K. A. & Cui, T. Carbon nanotube-based transparent thin film acoustic actuators and sensors. *Sens. Actuators A* **132**, 626–631 (2006).
54. Sharifzadeh Mirshekarloo, M. et al. Transparent piezoelectric film speakers for windows with active noise mitigation function. *Appl. Acoust.* **137**, 90–97 (2018).
55. Qiu, X. et al. Fully printed piezoelectric polymer loudspeakers with enhanced acoustic performance. *Adv. Eng. Mater.* **21**, 1900537 (2019).
56. Bolzmacher, C., Benbara, N., Rebillat, M. & Mechbal, N. Piezoelectric transducer for low frequency sound generation on surface loudspeakers. *IX ECCOMAS Thematic Conference on Smart Structures and Materials* 1–10 (2019).
57. Ohga, J. A flat piezoelectric polymer film loudspeaker as a multi-resonance system. *J. Acoust. Soc. Jpn.* **4**, 113–120 (1983).
58. Xiao, L. et al. Flexible, stretchable, transparent carbon nanotube thin film loudspeakers. *Nano Lett.* **8**, 4539–4545 (2008).
59. Suk, J. W., Kirk, K., Hao, Y., Hall, N. A. & Ruoff, R. S. Thermoacoustic sound generation from monolayer graphene for transparent and flexible sound sources. *Adv. Mater.* **24**, 6342–6347 (2012).
60. Niskanen, A. O. et al. Suspended metal wire array as a thermoacoustic sound source. *Appl. Phys. Lett.* **95**, 163102 (2009).

ACKNOWLEDGEMENTS

J.Z. acknowledges the funding support from the Science and Technology Development Fund, Macau SAR (FDCT) (File No. 0059/2021/AFJ, 0040/2021/A1), and University of Macau (MYRG-GRG2023-00041-FST-UMDF, MYRG2022-00003-FST, SRG2021-00001-FST). Y.M. acknowledges the funding support from Hong Kong Research Grants Council (25228722). I.M.L. acknowledges the Start-up Research Grant from the University of Macau (SRG2022-00038-FST) and the funding support from FDCT (File No. 0119/2022/A3).

AUTHOR CONTRIBUTIONS

Y.P. designed the prototypes and setups; performed the experiments; and wrote the original draft. Q.L. built the model for COMSOL simulation; assisted the experiments; and wrote the original draft. Z.L. and D.Z. assisted the experiment. K.Z. and Z.L. investigated related works. B.Z. and I.M.L. reviewed and edited the paper. Y.M. and J.Z. directed the research and revised the paper.

COMPETING INTERESTS

The authors declare no competing interests.

ADDITIONAL INFORMATION

Supplementary information The online version contains supplementary material available at https://doi.org/10.1038/s41528-023-00278-9.

Correspondence and requests for materials should be addressed to Yuan Ma or Junwen Zhong.

Reprints and permission information is available at http://www.nature.com/reprints

Publisher's note Springer Nature remains neutral with regard to jurisdictional claims in published maps and institutional affiliations.